NASA/TM-20250009589



Feasibility study report for 3D cloud tomography from space using passive microwave technologies

Jie Gong, Carey Johnson, Dong L. Wu, Sarah Ringerud, Ian Adams, Rachael Kroodsma

NASA Goddard Space Flight Center, Greenbelt, MD 20771

Yuli Liu

University of Maryland at Baltimore County, Baltimore, MD 21250

Mircea Grecu

Morgan State University, Baltimore, MD 21251

NASA STI Program Report Series

Since its founding, NASA has been dedicated to the advancement of aeronautics and space science. The NASA scientific and technical information (STI) program plays a key part in helping NASA maintain this important role.

The NASA STI program operates under the auspices of the Agency Chief Information Officer. It collects, organizes, provides for archiving, and disseminates NASA's STI. The NASA STI program provides access to the NTRS Registered and its public interface, the NASA Technical Reports Server, thus providing one of the largest collections of aeronautical and space science STI in the world. Results are published in both non-NASA channels and by NASA in the NASA STI Report Series, which includes the following report types:

- TECHNICAL PUBLICATION. Reports of completed research or a major significant phase of research that present the results of NASA Programs and include extensive data or theoretical analysis. Includes compilations of significant scientific and technical data and information deemed to be of continuing reference value. NASA counterpart of peer-reviewed formal professional papers but has less stringent limitations on manuscript length and extent of graphic presentations.
- TECHNICAL MEMORANDUM.
 Scientific and technical findings that are preliminary or of specialized interest,
 e.g., quick release reports, working
 papers, and bibliographies that contain minimal annotation. Does not contain extensive analysis.
- CONTRACTOR REPORT. Scientific and technical findings by NASA-sponsored contractors and grantees.

- CONFERENCE PUBLICATION.
 Collected papers from scientific and technical conferences, symposia, seminars, or other meetings sponsored or co-sponsored by NASA.
- SPECIAL PUBLICATION. Scientific, technical, or historical information from NASA programs, projects, and missions, often concerned with subjects having substantial public interest.
- TECHNICAL TRANSLATION.
 English-language translations of foreign scientific and technical material pertinent to NASA's mission.

Specialized services also include organizing and publishing research results, distributing specialized research announcements and feeds, providing information desk and personal search support, and enabling data exchange services.

For more information about the NASA STI program, see the following:

 Access the NASA STI program home page at http://www.sti.nasa.gov

NASA/TM-20250009589



Feasibility study report for 3D cloud tomography from space using passive microwave technologies

Jie Gong, Carey Johnson, Dong L. Wu, Sarah Ringerud, Ian Adams, Rachael Kroodsma

NASA Goddard Space Flight Center, Greenbelt, MD 20771

Yuli Liu

University of Maryland at Baltimore County, Baltimore, MD 21250

Mircea Grecu

Morgan State University, Baltimore, MD 21251

National Aeronautics and Space Administration

Goddard Space Flight Center Greenbelt, MD

The use of trademarks or names of manufacturers in this report is for accurate reporting and does not constitute an official endorsement, either expressed or implied, of such products or manufacturers by the National Aeronautics and Space Administration.
Available from:
NASA STI Program / Mail Stop 050 NASA Langley Research Center Hampton, VA 23681-2199

1. Executive Summary

Passive microwave (PMW) remote sensing technologies advanced rapidly in the past decade or so, making 3D cloud tomography (CT) increasingly feasible using PMW sensors. However, current 3D-CT study still dominantly concentrated at visible/infrared bands, which works well for thin clouds, but is limited to only outlining thick cloud boundaries. Despite being able to penetrate through thick clouds and to reveal the internal mass distribution, which is critical for precipitation forecast, there is no trade-space study readily available for MW/sub-mm radiometers for 3D-CT. Technology-wise, emerging new technologies can potentially enable hydrometeor profiling through tomography with a single sensor, but a thorough evaluation of feasibility and challenges is still missing.

This feasibility assessment report aims at addressing this gap from both science and technology perspectives. For science, we will use a simulated cloud case to present the trade-space study results focusing on **optimal vertical resolution** that can be achieved using different combinations of PMW instrument parameters. For technology, we will present our evaluation of candidate architectures, subsystem components, the desired specs, challenges and recommendations for future development directions. For disclaimer, this report is not intended as a comprehensive review, but rather as a starting point to kick-off more studies in this area.

2. Problem Description and Background

Profiling cloud vertical mass distribution, especially for thick clouds, is critical for accurate precipitation forecasting and understanding atmospheric processes (e.g., hydrological cycle). Consensus has been reached that active sensors such as cloud profiling radar (e.g., CPR) and lidar (e.g., CPL) are the best state-of-the-art (SOA) remote sensing instruments for cloud profiling with high vertical resolutions. However, their sparse observations significantly limit their applications to improving weather monitoring or forecasting, and the cost and shorter lifespan are amongst the major bottlenecks for launching more spaceborne active sensors or building ones with wider swaths to enhance the spatial sampling.

Synergizing multi-angle observations from spectrometers or spectrometer-polarimeters can reveal information about cloud 3D structures. The reconstruction of 3D cloud structures, namely "cloud tomography" (CT), was initially proposed back in 1980s [Warner et al., 1985] using two ground-based PMWs for a non-precipitating liquid cloud layer. Other than a later improvement of radiative transfer (RT) and microphysics modeling in Huang et al. [2008], 3D-CT reconstruction was studied dominantly in the visible-infrared (VIS/IR) domain ever since, mainly because of the booming of spaceborne spectrometer and polarimeter missions (e.g., Forster et al., 2021), the advancement of simulation RT through clouds (e.g., Levis et al., 2015, 2021) and inversion methods (e.g., Rogers, 2000; Kimes et al., 2009; Ido et al., 2023), as well as the rapid growth of computational power. Along this direction, a dedicated mission called CloudCT is proposed to be launched in 2026, which consists of a series of nanosats (Tzabari et al., 2022; concept shown in Fig. 1 below).



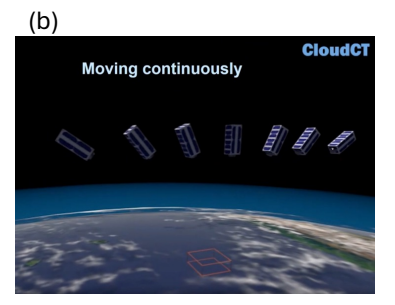
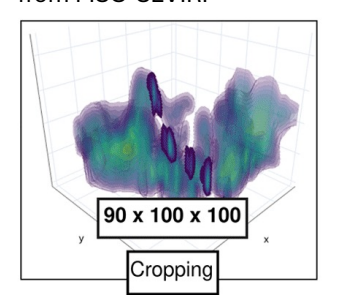


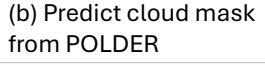
Figure 1: CloudCT mission (a) instrument concept (b) orbital distribution concept of seven 3U nanosats (adapted from https://www.nanosats.eu/sat/cloudct).

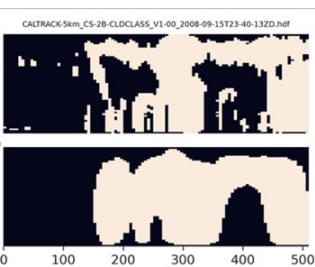
After entering the artificial intelligence (AI) era, decent number of studies emerge using different

machine learning (ML) techniques to predict cloud 3D structures from spectrometer/polarimeter images, which are often trained with collocated sparse spaceborne CPR or CPL profiles (e.g., Wang et al., 2023; Bruning et al., 2024; Foley et al., 2024; 2025; Amell et al., 2024). Fig. 2 presents some examples. The majority of peer-reviewed published ML 3D cloud reconstruction works focus on reconstructing the cloud boundaries (i.e., 3D masks) or types (e.g., cirrus, stratocumulus, etc.).

(a) Predict radar reflectivity from MSG-SEVIRI







(c) Predict ice water content from global merged IR dataset

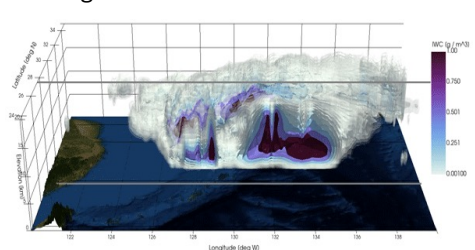


Figure 2: Three ML examples of 3D-CT using (a) MSG-SEVIRI spectrometer (Bruning et al., 2024); (b) POLDER polarimeter (Foley et al., 2024); and (c) global merged IR radiance dataset (Amell et al., 2024).

However, the limitation of what visible/IR bands can see is poorly considered or constrained in the ML works. Theoretically speaking, the penetration depth inside clouds cannot go beyond optical depth $\tau \sim 10$ (equivalent liquid or ice water path $\sim 100~g/m^2$) for visible + near IR and thermal IR bands (King et al., 1997), and multi-angle view 3D-CT cannot improve the penetration depth but rather constraining the cloud information close to the cloud boundaries from different view-angles. For a thick cloud, this will result in the so-called "Veiled Core" problem as shown in Fig. 3 below from Davis et al. (2021). A recent presentation (Forster et al., 2024) provides a more comprehensive trade-space study for 3D-CT using visible/IR channels, which recommended 9 views with maximum view angle of 70° to achieve smaller than 50 m vertical resolution for **thin PBL** clouds. Therefore, although ML demonstrated superior performance and great potential over traditional physical-based retrieval algorithms, their "retrieval" for optically thick clouds is essentially extrapolating mean structures of certain cloud features learnt from the supervised "truth" from active sensors.

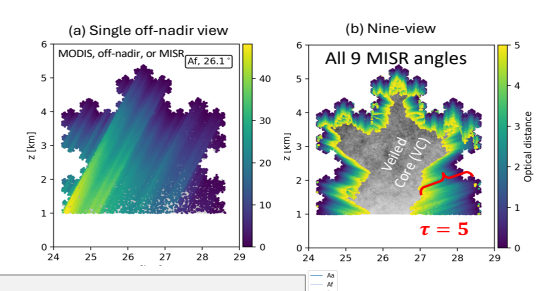


Figure 3: Theoretical calculation of optical penetration depth for spectrometer visible bands using (a) one offnadir view, mimicking what MODIS can see, and (b) 9-views, mimicking what MISR can see. While neither of them can see through a cloud with optical depth > 5, single-view can only constrain information near the boundary of cloud along the line-of-sight (LOS). Adapted from Davis et al. (2021).

Passive microwave (PMW) remote sensing technologies advanced rapidly in the past decade or so. In particular, the significant reduction of Size, Weight, Power and Cost (SWAP-C) enables the small-sat low-Earth orbit (LEO) constellation (e.g., the TROPICS mission); the hyperspectral capability adds more information content about cloud in the water vapor lines; and technology readiness level (TRL) enhancement for polarized filter detector and expansion to sub-millimeter (sub-mm) regime allow for detecting more detailed microphysical properties from clouds. All these technology developments are making 3D-CT increasingly feasible using PMW sensors. However, up till this point there are only a few

studies exploring cloud profiling capabilities using PMW sensors (e.g., Liu et al., 2018; May and Eriksson, 2025). Liu and Adams (2024) pioneers the first exploration on 2D-CT using MW and sub-mm bands, where they used a case study to prove the scientific merits without further investigating theoretical grounds.

With the support from a Goddard Space Flight Center (GSFC) internal research seed funding and leveraging the pironeer work from Liu and Adams (2024), this project strives to fill in the theoretical gap to link the PMW instrument specifications with vertical resolution that is physically achievable, or the so-called scientific traceability matrix (STM). Since the preferred instrument parameters can be readily achieved through a distributed smallsat/cubesat constellation, this report spearheaded in studying the possibility of a single PMW instrument architecture with subsystem TRL assessment. Although far from a comprehensive assessment report, we hope results and suggestions shared in this report can help initiate or facilitate future scientific and technology development efforts toward 3D-CT or cloud profiling using PMW(s) as a much cheaper substitute of spaceborne radar to enable cost-effective manufacturing and launching for the ultimate goal of improving accuracy of extreme weather monitoring and forecasting.

3. Science Trade Study

The science trade-space study is designed around the sensitivity of theoretical **vertical resolution** to two parameters: **number of views** and **view angles**. As our current effort largely leverages Liu and Adams (2024)'s framework, the sensitivity to channel frequency is not touched upon. We also didn't inspect the impact of footprint size, as it is dominantly constrained by antenna size and subsequently subject to cost caps.

3.1 Data and Methodology

A thick ice cloud case is selected from a CloudSat/CALIPSO transect on May 6, 2008, which is identical to Liu and Adams (2024). The IWP ranges between $100-4000g/m^2$ in this scene, which is well beyond the maximum sensitivity range for VIS/IR frequencies. The ground truth ice water content (IWC) profile from the joint CloudSat/CALIPSO 2C-ICE product (Fig. 4a) suggests a thick deck of ice cloud extending from freezing level at ~ 3 km up to ~ 11 km in altitudes with vertical resolution of 250 m and horizontal resolution of ~ 1.4 km.

NASA's Configurable Scanning Submillimeter-wave Instrument/Radiometer (CoSSIR) channels are selected for the forward simulation. The channel frequencies and noise level (NeDT) are listed in Table 1. Note that the polarization signatures are available for all CoSSIR channels, which have been demonstrated to help further constrain cloud parameters, but are not considered in the current study. The atmospheric radiative transfer simulator (ARTS) is employed for generating the simulated brightness temperatures (TBs) at CoSSIR channels. The retrieval procedure follows a Bayesian Monte Carlo Integration (BMCI) plus optimal estimation method (OEM) framework, detailed in Liu and Adams (2024). The flight parameters during NASA's IMPACTS (Investigation of Microphysics and Precipitation for Atlantic Coast-Threatening Snowstorms, McMurdie et al., 2022) campaign is used for simulating CoSSIR along-track scan patterns across this cloud deck, resulting in a consistent 125 different view-angles for almost every pixel (1.4 km X 250 m voxel size) except at two side boundaries (outmost view-angle = 50°). The contrast retrieval results for IWC vertical distribution between Fig. 4b (nadironly) and Fig. 4c (2D-CT) can clearly demonstrate the merit of using multi-angle views to accurately reproduce the detailed mass distribution structure within this thick cloud layer, while the nadir-only retrieval shows "striping" effect, which is also reported by May and Eriksson (2025).

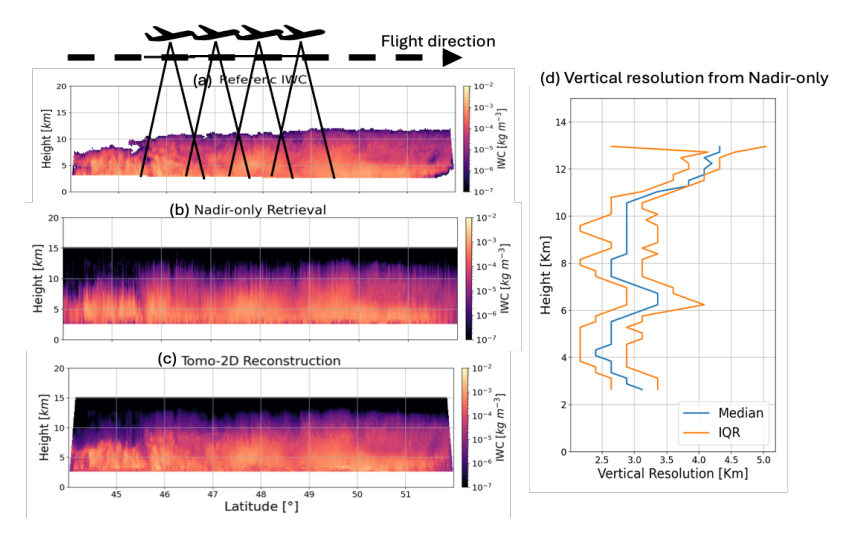


Figure 4: The thick ice cloud case from a transect of CloudSat/CALIPSO on May 6, 2008. (a) is the combined radar + lidar retrieval from the 2C-ICE product, serving as the ground truth; (b) retrieval from CoSSIR instrument nadir-view experiment; (c) retrieval from 2D tomographic (Tomo-2D) retrieval where each voxel is observed from 125 different views; (d) mean vertical resolution that theoretically can be achieved using the nadir-only retrieval (median in blue, and 1st and 3rd quartiles in orange to bound the variations). Panel (a) (b) and (c) are adapted from Liu and Adams (2024).

Table 1: Channel frequency assumption.

Frequency (GHz)	170.5	177.31	180.31	182.31	325.15 ± 11.5	325.15 ± 3.4	325.15 ± 0.9	684
NeDT (K)	0.2	0.2	0.2	0.2	1.5	1.5	1.5	1.0

Theoretical achievable vertical resolution is computed using the averaging kernel (AK) method. AK is defined as the sensitivity of a retrieval \hat{x} to the true state x:

$$AK = \frac{\partial x}{\partial x} \tag{1}$$

Where $\hat{x} = x_a + AK \cdot (x - x_a)$, with x_a being the first guess from the apriori database. AK characterizes the sensitivity of a retrieval at a given height to the adjacent levels. Hence the full-width at half maximum (FWHM) of the AK is a good estimation of the vertical layer thickness where two adjacent layers can be considered independent of each other. According to Rogers (2000), the AK method is valid for quasilinear relationship, meaning that this method is less trustworthy close to cloud top, bottom or for thin cloud scenes.

Applying the AK method to this case, we can find the nadir-only retrieval can only achieve 2.5 – 3.5 km vertical resolution on average (Fig. 4d). As a contrast, we can achieve the native 250 m vertical resolution of a spaceborne radar using the 2D-CT approach as the retrieval is over-constraint by 125 different views. This ideal situation can only occur for airborne or ground-based scanning.

3.2 Trade-space analysis results

For spaceborne PMWs, it is impossible to achieve 125 different views. Hence, we rerun this Observing System Simulation Experiment (OSSE) using different number of views and different view-angles settings to understand the trade-space behavior. The averaged vertical resolution is displayed as a function of number of view-angles (y-axis) and view angles (x-axis) in Fig. 5. As expected, we can achieve better vertical resolution with more views from different angles, and slantwise view always performs better than a near-nadir view. The cloud top and bottom are the poorest constrained, associated with degraded

vertical resolutions. However, such an issue can be largely mitigated through using a slantwise view, as shown in Fig. 6. In an extreme situation, if we only have two co-flying PMW on the same orbit, pointing fore and aft to the same swath, 1-1.5 km vertical resolution can be stably achieved according to Fig. 5, which is already much better than 2-3.5 km vertical resolution from a single PMW radiometer. If the CloudSat 0.25 km vertical resolution is expected, we need a distributed system of 8 or more identical PMWs each tilt at different angles. This is still cost-effective as CloudSat mission costs about \$217 million for building the radar and the launch service (inflation adjusted), while Earth Venture TROPICS mission cost is about \$30 million for 4 satellites in 2 launches. However, additional propulsion systems haven't been factored in the latter scenario to maintain a stable separation and fixed tilt angles in the same orbit, which adds cost burden and risks. In the following section, we will discuss the feasibility of a single radiometer design that can achieve multiple view-angles using one instrument.

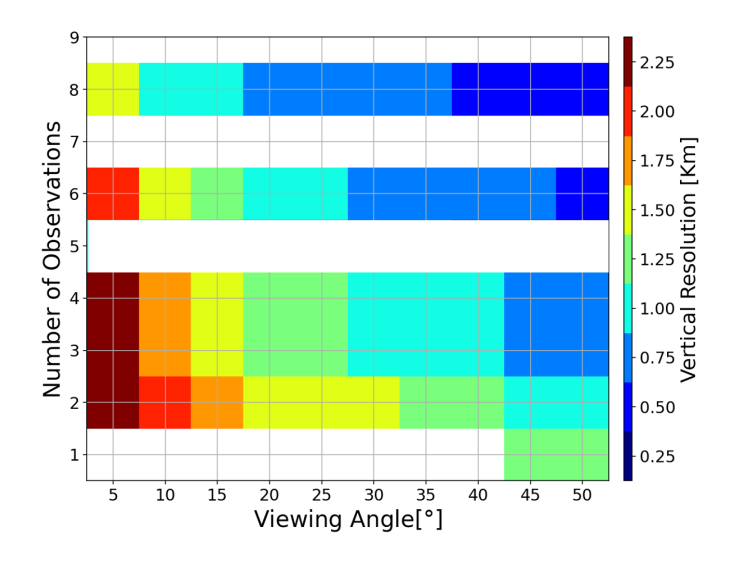


Figure 5: Averaged vertical resolution across the cloud scene shown in Fig. 4a as a function of number of views (y-axis) and view angles (x-axis) for along-track scan. OSSE experiments were only conducted in colored grids.

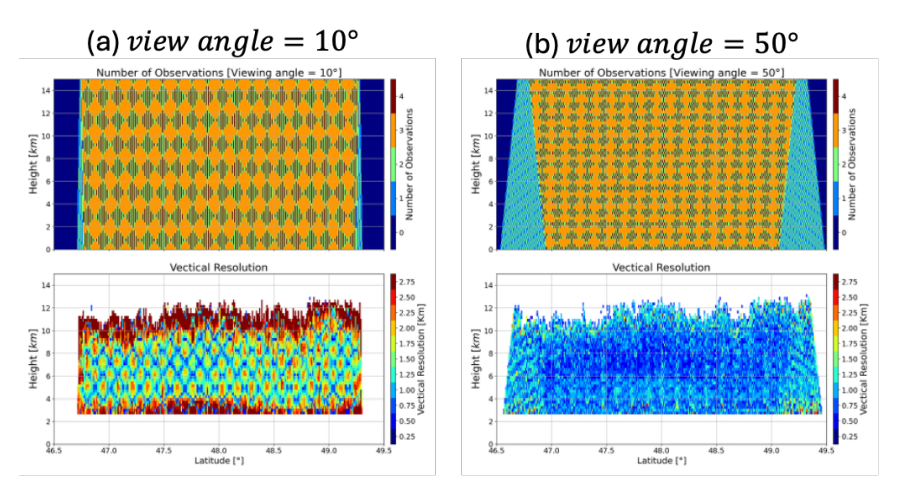


Figure 6: Vertical resolution distribution across the cloud deck for three views with view-angle at (a) 10° and (b) 50°. One can see a slantwise view is critical for achieving a better and homogeneous CT performance.

4. Technology Survey

4.1 Candidate Architecture Study

The technological goal is to design a system that is suitable for Small-Sat vehicles. This desire requires a system where SWAP-C considerations are paramount. The baseline instrument will be capable of scanning at least three simultaneous look angles according to the STM in Fig. 5. The instrument viewing geometry demonstration is shown in Fig. 7. The optimum view-angle is a part of this trade-study and has been discussed in the previous section. There are many possible hardware configurations which can be utilized to obtain three simultaneous look angles. Since the backend subsystems have reached relatively high TRL (Table 2 for a TRL assessment), we will focus on discussing possible frontend solutions and their individual challenges in this report.

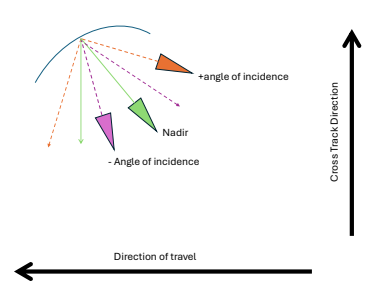


Figure 7: Instrument view angle illustration assuming three simultaneous views (fore, nadir and aft).

System	Subsystem	TRL	Examples
Frontend	Dichroic Splitters\Filters	PoLSIR	
	Grid Polarizers	6	PoLSIR
	Feedhorn 89 GHz	9	ATMS,CoSMIR
	Feedhorn 183 GHz	9	ATMS,CoSMIR
	Feedhorn 325 GHz	6	CoSSIR,PoLSIR,TWICE, TROPICS
	Feedhorn 684 GHz	6	PoLSIR, TWICE
Receiver	Receiver 89 GHz	9	ATMS, CoSMIR, TWICE, TROPICS
	Receiver 183 GHz	9	ATMS, CoSMIR, TWICE, TROPICS
	Receiver 325 GHz	6	CoSSIR\PoLSIR\TWICE, TROPICS
	Receiver 684 GHz	6	PoLSIR, TWICE
BackEnd Digital Electronics		6	CoSSIR\PoLSIR\TWICE, TROPICS

Table 2: TRL levels for accompanying subsytems

The trade-space for frontend candidates evaluated mechanisms capable of producing three simultaneous look angles: (1) Reflector/Feedhorns; (2) Risley Prisms; (3) Rotatable Planar Phase Shifting Surfaces (RPPSS); and (4) Reconfigurable Reflect Arrays.

If we chose to use the common Reflector/Feedhorn configuration, we would then need three feedhorns per frequency band at three different look angles at a minimum, for a total of **nine feedhorns**. Additionally, the size of the antenna aperture will need to be slightly increased into a Parabolic-Torus configuration. This automatically increases the mass and weight of the system. The increase in mass makes the Reflector/Feedhorn configuration less desirable for this application. Multi-look angles can also be achieved with a mechanically steering a single feedhorn and/or reflector system. However, mechanical scanning is discouraged for spaceborne sensors because high scanning speeds are required to achieve sufficient system integration time.

The feedhorn frontends can be replace with a Risley Triple Prism (Ostaszewski et al., 2006), or RPPSS. A Risley prism configuration consists of a pair of stacked wedged prisms (McEwen et al.1984). The steering angle of the prism is determined by the positional alignment of the wedged prisms. A separate Risley prism is needed for each operating frequency of the system. The scan angle direction is generated by mechanically rotating the prisms. The design of the wedged material is simple. However, the design of the mechanical system and the associated control hardware could prove to be power prohibitive, heavy, and thermally unstable. The RPPSS (e.g. Gagnon et al., 2010) is also capable of producing multiple look angles but is not a desirable method due the need for mechanical gearing to quickly spin the metalized mechanism. Spinning the mechanism will require a more sophisticated counter momentum compensator on the satellite platform, thus adding more weight to the system. The same shortcomings can be said for Spinning Metal Disks (SMD) antenna which is also mechanically controlled. This antenna type is not explored in this study.

The final antenna explored in this study is a Reconfigurable Antenna (e.g., Berry et al. 1963; Yang et al. 2016; Chou et al. 2023). Reconfigurable Antennas (RA) can be reconfigured via frequency, polarization, or radiation pattern. For our purposes, we investigated the radiation pattern reconfigurability. The radiation pattern is reconfigured by altering the phase front of the propagated signal, similar to a Phased Array Antennas. RA meets the SWAP-C of a stand-alone satellite system and can achieve the multi-look angle requirement. Specifically, we believe a planar meta-surface antenna is a viable solution in a Reconfigurable Reflect Array (RRA) arrangement. This system's propagation parameters can be dynamically reconfigured, or configured for predefined simultaneous scan angles. Also, it is possible to use a meta-surface feed-system for further diversity. Currently the proposed RRA will be illuminated by feedhorns tuned to the appropriate frequency bands to ensure integration time equivalent to a traditional scanning reflector while also achieving the necessary along-track angles and swath coverage.

The RRA consists of patch elements as the radiators that are controlled using pin diodes, microelectromechanical systems (MEMS), or varactors. The phase shift is achieved by selectively switching on/off the patch elements, thus achieving beam steering. In the proposed configuration, the pin diodes should suffice because the system is low power, using fixed look angles, and the expected switching speed is in the microseconds range. MEMS may require higher currents than pin diodes. Varactors are usefully for varying the phase shift in a continuous scanning configuration.

The planar panel is recommended for the RRA architecture, which requires careful configuration for minimizing risk and optimizing performance. These planar panels can suffer lower radiation efficiency as compared to their metalized parabolic-toroidal counterparts. However, the planar panel (as opposed to parabolic reflector) is favorable due to low profile, lower weight, and ease of deployment. The size of the planar panel aperture is dependent on the gain, beamwidth, flight altitude, and desired footprint size. All these parameters will need to be defined by the mission before final design considerations. Based on our gain estimations (Table 4), we believe that apertures between **0.5 to 1m** will suffice. A single panel is designed by the MIT Lincoln Labs' Configurable Reflectarray Wideband Scanning Radiometry (CREWSR) instrument team for lower MW frequencies (Blackwell et al., 2023). However, it should be recognized that fabricating one single panel with integrated elements at multiple frequencies requires tight tolerances in the patch element fabrications. Another complication is the potential coupling between the elements. Also, the active switching elements and their associated signal traces are yet another design

challenge. Using Fig. 8b for a two-frequency RRA configuration as an example demonstration for integrated patch elements, each additional frequency band will require additional integrated patch elements tuned to the resonant frequency band. Fig. 8a illustrates a probable control circuitry design. One can find the potential of significant amount of crosstalk between the different frequency bands. The integrated control circuitry will mostly likely be intricately cumbersome. If successfully demonstrated in CREWSR, the planar panel circuitry design there can be extended to our frequencies here with added number of elements for an anticipated smaller antenna and smaller footprint size at sub-mm frequencies.

Table 3: Total elements estimated for different frequencies with a 0.5m panel dimension assumption. This is in the similar range with Blackwell et al. (2023) for 23 - 58 GHz.

Frequency(Ghz)	89	183	325
Wavelength (λ) (m)	0.00337	0.00164	0.00092
Element			
Spacing(~λ/2) m	0.00168	0.00082	0.00046
x dimension (m)	0.500	0.500	0.500
Sampling angle			
degrees(0)	45	45	45
Optimum Element Δ			
Spacing (m)	0.0024	0.0012	0.0007
# Elements in one axis	210	432	767
Total # Elements	44,067	186,308	587,618

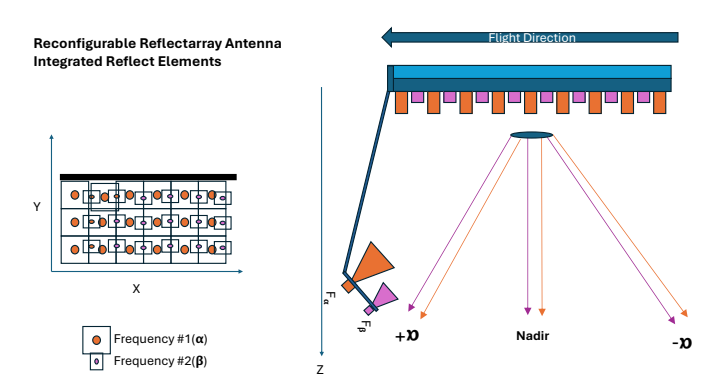


Figure 8: (a) A possible diode circuit layout for a single-panel RRA configuration, (b)RRA with integrated two frequency patch elements, which is the CREWSR solution.

Table 4: Projected Gain based on the number of Array Elements within the prescribed Aperture Diameter

Aperture Diameter(m)	Element Gain (dBi)	Efficiency (%)	89 GHz	183 GHz	325 GHz	684 GHz
0.50	6.00	100	52.44	58.70	63.69	70.15
1.00	6.00	100	58.46	64.72	69.71	76.18

1.50	6.00	100	61.98	68.24	73.23	79.70
2.00	6.00	100	64.48	70.74	75.73	82.20

Considering the caveats and associated risks of the integrated planar panel design, Fig. 9 is our recommended configuration. Fig. 9 separates the two frequency bands (89 and 183 GHz considered here) into two separate planar-panel antennas. The planar panels are simpler in construction and simpler to deploy while maintaining surface flatness. The control circuitries are also separated; thus, less complicated and reduces potential crosstalk between the different bands of operation.

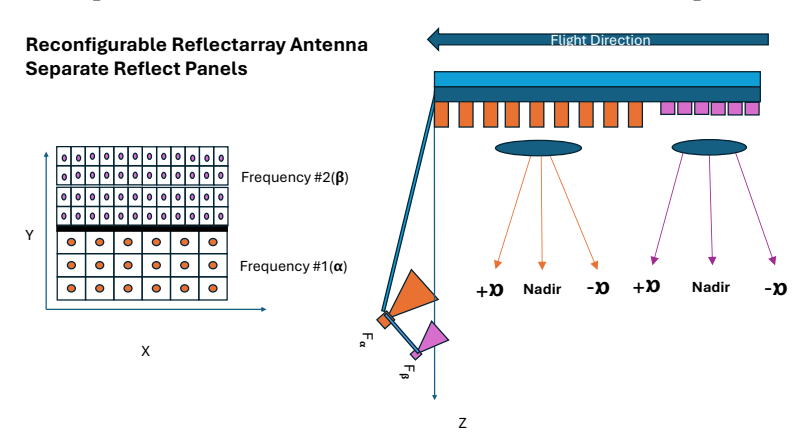


Figure 9: Two Frequency RRAs - separated planar panels, which is the recommended solution

In summary, the recommended physical frontend/antenna configuration is to use Reconfigurable Reflect Arrays. Each frequency band of operation will be configured on individual panels. Planar panels using beam forming arrays will meet the SWAP-C for satellite operations (Yurduseven et al., 2021; Wu et al., 2022).

4.2 Relevant State of Art (SOA) technologies at the backend

Some technology advancements at the backend are instrumental for the possibility of a (series of) smallsat PMW-CT mission. In this section a brief overview of these technologies.

Firstly, the compact Monolithic Microwave Integrated Circuit (MMIC) has now been widely adopted in reducing SWAP-C for smallsat/cubesat missions (e.g., TEMPEST-D, TROPICS). Further reduction of SWAP-C can now be realized through more advanced narrow-band filter for direct detector receiver enabled by the advanced 25-nm indium phosphide (InP) high-electron-mobility transistor (HEMT) for 200 GHz and below (Leuther et al., 2021) and 243 and 684 GHz (Wu et al., 2019a, 2019b). The 1/f noise issue at 684 GHz (Yoon et al., 2017) can be mitigated using the method developed in Ogut et al. (2021), although the latter has so far only been demonstrated in lab environment.

Secondly, the hyperspectral (HMW) capability realized through Application-Specific Integrated Circuit (ASIC) and Photonic Integrated Circuit (PIC) is expected to provide more information content about cloud vertical structure, especially within the planetary boundary layer (PBL). NASA is currently building a pathfinder spaceborne HMW instrument – AURORA – to elevate the TRL to 7 and above.

Lastly, hydrodyne radiometer-polarimeter will be demonstrated TRL 7 and above by the upcoming PolSIR mission. Incorporating with VDI filters, the robust polarization measurements will enable more sensitivity to cloud microphysics and hence better constrain of cloud vertical structure retrieval. Further, narrow-band filter fabrication has reached mature level to integrate with direct detector receivers for next-

generation radiometer-polarimeters.

These are all technologies in parallel that PMW-CT instrument can greatly leverage on.

4.3 Cost Barrier and Recommendation for Future Development

The CREWSR instrument and our proposed system face similar challenges in the availability of the switching components and the vast number of required for a single RRA. Today a pin diode in the 70 – 100 GHz range is in the tens of dollars range. Just to populate the RRA will cost approximately \$0.5M for 89 GHz and up to \$6M for 325GHz with 0.5 m length assumption. This cost is not favored for higher-frequency channels currently. Use of innovative materials (e.g., Kim et al., 2024) or cost-effective packaging are among some of the mitigation strategies that warrant further in-depth investigation. As semiconductor development advances at a fast pace because of the increased market size, we foresee a consistent decreasing trend for per device cost. We would also encourage development in radiometer topology to handle multiple feed inputs, which can be used to support either a traditional reflector or an RRA.

4.4 Alternative Technology Options

Distributing a series of smallsat radiometers is a most viable solution for PMW-CT with current technologies (e.g., TROPICS). Emerging efforts in the commercial space, such like the TMS (Tomorrow Microwave Sounder, heritage of TROPICS radiometers) constellation, has been starting to demonstrate not only the TRL, but also the value of the business model for leveraging industry capabilities for PMW-CT and ultimate enhancement of extreme weather monitoring and forecast.

Some current low TRL technologies might worth more explorations. These include Phase Shifting Surfaces (PSSs), Holographic Metasurface Antenna (HMA), and Parallel-Plate Lens (PPL) antennas.

PSSs change the phase of the incoming wavefront by passing the wavefront through multiple lattices of varying shapes etched into sheeting of dielectric material. The choice of shapes, dielectric materials, metal surfaces, and material thicknesses are all part of the design space. Designing PSSs is very challenging due to the extensive full-wave simulations needed to characterize the complex, multi-layer structures and their interaction with the electromagnetic waves (Biswas et al., 2023). HMA borrows techniques developed in optics. It is an emerging technology for passive microwave radiometry, offering advantages like a low profile, reduced complexity, and enhanced performance over traditional mechanically scanned systems. HMA is currently receiving attention in 6G network development (e.g., Omen et al., 2025). The PPL design was proposed decades ago, and regained interests in recent years in the 5G communication domain. It has been demonstrated viability at Ka band (Fonseca et al., 2021). Further research is warranted for investigating the applicability of HMA and PPL to PMW remote sensing, as well as extendibility to sub-mm domains.

5. Conclusion and Outlook

This report delivers our preliminary study results of a spaceborne passive-microwave radiometer (PMW) mission concept that can be dedicated to cloud tomography (3D-CT). Our study contains both the science aspects and technology survey. For science, we deliver the first science traceability matrix (STM) of the instrument parameters to realize vertical profiling capability of thick clouds that is comparable to that from the CloudSat radar. For technology aspect, we investigated several possible front-end solutions. Among all viable antenna candidates, we recommend Reconfigurable Reflect Array (RRA) for future development, recognizing both the merits and caveats/gaps. A top-level review is also given to State-of-the-Art (SOA) backend technologies that can be leveraged upon for building a smallsat multi-angle PMW. It is pointed out that one stand-alone instrument is not necessarily the only solution. A distributed system leveraging the instrument and business models from the commercial space might also be a cost-effective solution as well.

Although far from a comprehensive assessment report, we hope pioneering results and suggestions shared in this report can help initiate or facilitate future scientific and technology development efforts toward 3D-CT or cloud profiling using PMW(s) as a much cheaper substitute of spaceborne radar to enable cost-effective manufacturing and launching for the ultimate goal of improving accuracy of extreme weather monitoring and forecasting. There are many dimensions of trade-space parameter that need to be studied in the future, including but not limited to channel frequencies, hyperspectral versus heritage bands, and the benefit of introducing polarimetry measurements. In PMW regime, surface emissivity represents a large and dynamic contribution to the wings of the absorption band and window bands (Ringerud et al., 2015). Emissivity retrieval for certain surface types (e.g., snow or ice-covered surfaces, deserts) is especially sensitive to viewing angles, and tomographic retrieval would bring added value to the development of more complex surface models and retrieval schemes that will be increasingly important for future missions or weather applications over complicated surfaces.

Reference:

Amell, A., Pfreundschuh, S., and Eriksson, P. (2024): The Chalmers Cloud Ice Climatology: retrieval implementation and validation, Atmos. Meas. Tech., 17, 4337–4368, https://doi.org/10.5194/amt-17-4337-2024

Berry, D. G., R G. Malech, W. A. Kennedy (1963): The Reflectarray Antenna, IEEE Transactions on Antennas and Propagation. Vol. 11, No.6, November 1963, 645 – 651, https://doi.org/10.1109/TAP.1963.1138112

Biswas, A., Zekios, C.L. & Georgakopoulos, S.V. (2023): An ultra-fast method for designing holographic phase shifting surfaces. Sci Rep 13, 16511. https://doi.org/10.1038/s41598-023-43815-2

Blackwell et al. (2021): New microwave radiometer technologies featured in the upcoming NASA TROPICS Pathfinder and Constellation Missions in 2021/2022, SPIE remote sensing, proceedings vol 11858, https://doi.org/10.1117/12.2600441

Blackwell, W., C. Kataria, W. Moulder, S. C. Reising and V. Chandrasekar (2023): New Technologies for Intelligent High-Resolution Sensing from Small Satellite Platforms: CREWSR and Video, IGARSS 2023 - 2023 IEEE International Geoscience and Remote Sensing Symposium, Pasadena, CA, USA, 2023, pp. 1112-1114, doi: 10.1109/IGARSS52108.2023.10283300

Baranauskas et al. (2025): A commercially available digital spectrometer ASIC, IEEE J. of selected topics in applied earth observations and remote sensing, 18, https://doi.org/10.1175/WAF-D-24-0221.1

Brüning, S., Niebler, S., and Tost, H. (2024): Artificial intelligence (AI)-derived 3D cloud tomography from geostationary 2D satellite data, Atmos. Meas. Tech., 17, 961–978, https://doi.org/10.5194/amt-17-961-2024

Chou, H. T., N. N. Wang, M. Fang, L. Q. Wang, P. Akkaraekthalin, D. Torrungrueng (2023): Dual-Band Reflectarray Antennas Using Integrated Resonant and Non-Resonant Natures of Metallic Waveguide Elements at Millimeter Wave Frequencies, Radio Science, 58, e2022RS007494, https://doi.org/10.1029/2022RS007494

Craig M. Wittenbrink, Glen G. Langdon Jr., and Gabriel Fernandez (1996): Feature extraction of clouds from GOES satellite data for integrated model measurement visualization, Proc. SPIE 2666, Image and Video Processing IV, https://doi.org/10.1117/12.234744

Davis, A., L. Forster, D. Diner (2021): A Necessary Step Toward Cloud Tomography from Space using MISR and MODIS: Understanding the Physics of Opaque 3D Cloud Image Formation. ESS Open Archive, March 12, 2021. https://doi.org/10.1002/essoar.10506476.1

- Foley, S. R., Knobelspiesse, K. D., Sayer, A. M., Gao, M., Hays, J., and Hoffman, J. (2024): 3D cloud masking across a broad swath using multi-angle polarimetry and deep learning, Atmos. Meas. Tech., 17, 7027–7047, https://doi.org/10.5194/amt-17-7027-2024
- Foley, S. R., Knobelspiesse, K. D. (2025): 3D cloud neural rendering, https://github.com/nasa/atmospheric-neural-rendering
- Fonseca, N.J.G., Liao, Q. and Quevedo-Teruel, O. (2021): Compact parallel-plate waveguide half-Luneburg geodesic lens in the Ka-band. IET Microw. Antennas Propag, 15: 123-130. https://doi.org/10.1049/mia2.12028
- Forster, L., A. B. Davis, D. J. Diner, and B. Mayer (2021): Toward Cloud Tomography from Space Using MISR and MODIS: Locating the "Veiled Core" in Opaque Convective Clouds. J. Atmos. Sci., 78, 155–166, https://doi.org/10.1175/JAS-D-19-0262.1
- Forster, L. et al. (2024): New Angles on the PBL: Potential and Limitations of Space-borne Atmospheric Tomography for Characterizing the Planetary Boundary Layer, AGU fall meeting 2024, Session: Atmospheric Sciences / Remote Sensing of the Planetary Boundary Layer from Ground, Air, and Space III Oral, id. A24G-07.
- Gagnon, N., A. Petosa, D. A. McNamara (2010): Thin Microwave Quasi-Transparent Phase-Shifting Surface (PSS), IEEE Transactions on Antennas and Propagation. Vol 58, No 4, April 2010, 1193 1201, https://doi.org/10.1109/TAP.2010.2041150
- Ido Czerninski, Yoav Y. Schechner (2023): PARS Path recycling and sorting for efficient cloud tomography. Intell Comput., 2:0007. doi:10.34133/icomputing.0007
- Huang, D., Y. Liu, and W. Wiscombe (2008): Determination of cloud liquid water distribution using 3D cloud tomography, J. Geophys. Res., 113, D13201, doi:10.1029/2007JD009133
- Kim, D. et al. (2024): High-Efficiency GaN Vertical PiN Diode Power Devices for Satellite Communications in 6G Networks, 2024 15th International Conference on Information and Communication Technology Convergence (ICTC), Jeju Island, Korea, Republic of, 2024, pp. 1490-1491, doi: 10.1109/ICTC62082.2024.10826709
- Kimes, D. S., Knyazikhin, Y., Privette, J. L., Abuelgasim, A. A., & Gao, F. (2000): Inversion methods for physically-based models. Remote Sensing Reviews, https://doi.org/10.1080/02757250009532396
- King, M., S.-C. Tsay, S. Platnick, M. Wang, and K.-N. Liou (1997): Cloud Retrieval Algorithms for MODIS: Optical Thickness, Effective Particle Radius, and Thermodynamic Phase, MODIS cloud algorithm ATBD, Collection 5, https://modis.gsfc.nasa.gov/data/atbd/atbd mod05.pdf
- Levis, A., Y. Y. Schechner, A. Aides and A. B. Davis (2015): Airborne Three-Dimensional Cloud Tomography, 2015 IEEE International Conference on Computer Vision (ICCV), Santiago, Chile, 2015, pp. 3379-3387, doi: 10.1109/ICCV.2015.386.
- Levis, A., Davis, A. B., Loveridge, J. R., & Schechner, Y. Y. (2021): 3D cloud tomography and droplet size retrieval from multi-angle polarimetric imaging of scattered sunlight from above. In Polarization Science and Remote Sensing X (Vol. 11833, pp. 31-45). SPIE, https://doi.org/10.1117/12.2593369
- Liu, Y., Buehler, S. A., Brath, M., Liu, H., and Dong, X. (2018): Ensemble Optimization Retrieval Algorithm of Hydrometeor Profiles for the Ice Cloud Imager Submillimeter-Wave Radiometer, J. Geophys. Res. Atmos., 123, 4594–4612, https://doi.org/10.1002/2017JD027892
- Liu, Y. and Adams, I. S.(2025): Tomographic reconstruction algorithms for retrieving two-dimensional ice cloud microphysical parameters using along-track (sub)millimeter-wave radiometer observations, Atmos. Meas. Tech., 18, 1659–1674, https://doi.org/10.5194/amt-18-1659-2025

- Leuther, A., L. John, R. Iannucci, T. Christoph, R. Aidam, T. Merkle, A. Tessmann (2021): InGaAs HEMT MMIC Technology on Silicon Substrate with Backside Field-Plate, 2020 50th European Microwave Conference (EuMC), Utrecht, Netherlands, 2021, pp. 187-190, doi:10.23919/EuMC48046.2021.9337957.
- May, E. and Eriksson, P. (2025): The Ice Cloud Imager: retrieval of frozen water mass profiles, EGUsphere [preprint], https://doi.org/10.5194/egusphere-2025-2190
- McEwen, C. D., M. R. Khan (1984): Beam Steering Method with Improved Sidelobe Response Using Dielectric Wedges for Satellite TV Reception, IEEE 1984 14th European Microwave Conference., 1984 14th European Microwave Conference, 19 March 2007, 681 685, https://doi.org/10.1109/EUMA.1984.333403
- McMurdie, L., Heymsfield, G., Yorks, J., Braun, S., SkofronickJackson, G., Rauber, R., Yuter, S., Colle, B., McFarquhar, G., Poellot, M., and Novak, D. (2022): Chasing snowstorms: The Investigation of Microphysics and Precipitation for Atlantic coast threatening snowstorms (IMPACTS) campaign, B. Am. Meteorol. Soc., 103, E1243–E1269.
- Ogut, M., C. M. Cooke, W. R. Deal, P. Kangaslahti, A. B. Tanner and S. C. Reising (2021): A Novel 1/f Noise Mitigation Technique Applied to a 670 GHz Receiver. IEEE Transactions on Terahertz Science and Technology, 11(1), 109-112.
- Omam, Z. R., Taghvaee, H., Araghi, A., Garcia-Fernandez, M., Alvarez-Narciandi, G., Alexandropoulos, G. C., ... & Khalily, M. (2025): Holographic metasurfaces enabling wave computing for 6G: Status overview, challenges, and future research trends. arXiv preprint arXiv:2501.05173.
- Ostaszewski, Miroslaw, S. Harford, N. Doughty, C. Hoffman, M. Sanchez, D. Gutow, R. Pierce (2006): Risley Prism Beam Pointer, Proc. Of SPIE, Vol. 6304, 630406, (2006) 0277-786X/06\$15, doi:10.1117/12.679097. https://www.spiedigitallibrary.org/conference-proceedings-of-spie/6304/1/Risley-prism-beam-pointer/10.1117/12.679097.full
- Rogers (2000): Inverse Methods for Atmospheric Sounding, World Scientific Publishing Co., https://doi.org/10.1142/3171
- Ringerud, S., C. D. Kummerow and C. D. Peters-Lidard (2015): A Semi-Empirical Model for Computing Land Surface Emissivity in the Microwave Region, IEEE Transactions on Geoscience and Remote Sensing, vol. 53, no. 4, pp. 1935-1946, doi: 10.1109/TGRS.2014.2351232.
- Tzabari, M., V. Holodovsky, O. Shubi, E. Eytan, I. Koren and Y. Y. Schechner (2022): Settings for Spaceborne 3-D Scattering Tomography of Liquid-Phase Clouds by the CloudCT Mission, in IEEE Transactions on Geoscience and Remote Sensing, vol. 60, pp. 1-16, 2022, Art no. 4109716, doi: 10.1109/TGRS.2022.3198525
- Wang Y., J. Gong, D. L. Wu, L. Ding (2023): Toward Physics-informed Neural Networks for 3D Multi-layer Cloud Mask Reconstruction, IEEE Transactions on Geoscience and Remote Sensing, https://doi.org/10.1109/tgrs.2023.3329649
- Warner, J., J. F. Drake, and P. R. Krehbiel (1985): Determination of cloud liquid water distribution by inversion of radiometric data, J. Atmos. Sci. Oceanic Technol., 2, 293–303.
- Wu, D. L., J. R. Piepmeier, J. Esper, N. Ehsan, P. E. Racette, T. E. Johnson, B. S. Abresch, E. Bryerton (2019a): IceCube: spaceflight demonstration of 883-GHz cloud radiometer for future science, SPIE Optical Engineering Applications, 2019, San Diego, CA, United States., 1113103 (2019) https://doi.org/10.1117/12.2530589

Wu, D. L., M. Vega, M. Solly, V. Marrero, K. Hart, S. Guerrero, W. Gaines, C. Du Toit, G. De. Amici, W. Deal, A. Dabrowski, M. Coon, R. Chipman (2019b), SWIRP (Submm-Wave and Long Wave Infrared Polarimeter); A New Tool for Investigations of Ice Distribution and Size in Cyrrus Clouds, IGARSS 2019 - 2019 IEEE International Geoscience and Remote Sensing Symposium, Yokohama, Japan, 2019, pp. 8436-8439, https://doi.org/10.1109/IGARSS.2019.8898230

Wu, Y., S. Yu, N. Kou, Z. Ding, Z. Zhang (2022): A Liquid Metal Based 1-Bit Reconfigurable Reflectarray Antenna for Beam-Scanning Applications, AEU _ International Journal of Electronics and Communications, Vol 165, June 2023, https://doi.org/10.1016/j.aeue.2023.154646

Yang, Huanhuan, F. Yang, S. Xu, Y. Mao, M. Li, X. Cao, J. Gao (2016): A 1-Bit 10 x 10 Reconfigurable Reflectarray Antenna: Design, Optimization, and Experiment, IEEE Transactions on Antennas and Propagation. Vol. 64, No.6, June 2016, 2246-2254., https://ieeexplore.ieee.org/document/7448838

Yoon, D., J. Kim, J. Yun, M. Kaynak, B. Tillack, J.-S. Rieh (2017): 300-GHz direct and heterodyne active imagers based on 0.13-µm SiGe HBT technology, IEEE Trans. THz Sci. Technol., vol. 7, no. 5, pp. 536-545.

Yurduseven, O., C. Lee, D. Gonzalez-Ovejero, M. Ettorre, R. Sauleau, C. Chattopadhyay, V. Fusco, and N. Chahat (2021): Multibeam Si\GaAs Holographic Metasurface Antenna at W-Band, IEEE Transactions on Antennas and Propagation. Vol. 69, No.6, June 2021, 3523 -3528, https://doi.org/10.1109/TAP.2020.3030898

The use of trademarks or names of manufacturers in this report is for accurate reporting and does not constitute an official endorsement, either expressed or implied, of such products or manufacturers by the National Aeronautics and Space Administration.